

---

# Effect of Mixed Modifiers on Electrical Mechanism of Zinc-Phosphate Amorphous Semiconducting Glass

---

<sup>1,2</sup>Arpan Mandal, <sup>3,\*</sup>Dipankar Biswas, <sup>4</sup>Rittwick Mondal, <sup>5</sup>Bidyut Kumar Ghosh, <sup>2</sup>Nipu Modak

<sup>1</sup> Mechanical Engineering Department, Regent Education and Research Foundation, Kolkata 700121, India

<sup>2</sup> Mechanical Engineering Department, Jadavpur University, Kolkata-700032, India

<sup>3,\*</sup> Electronics & Communication Engineering Department, Regent Education and Research Foundation, Kolkata 700121, India

<sup>4</sup>Chowhatta High School, Birbhum, West Bengal 731201, India

<sup>5</sup>Electrical Engineering Department, Regent Education and Research Foundation, Kolkata 700121, India

Email: [dipankar\\_aec@rediffmail.com](mailto:dipankar_aec@rediffmail.com)

## Abstract.

The impact of MoO<sub>3</sub> and TeO<sub>2</sub> inclusion on electrical and dielectric mechanisms of the zinc-phosphate host glass matrix has been reported in this communication. The well-known melt quenching route has been employed to produce glass nanocomposite systems. The formation of superimposed nanocrystallites of ZnMoO<sub>4</sub>, Mo<sub>5</sub>TeO<sub>16</sub> and TeO<sub>3</sub> within the amorphous glass matrix is established by XRD spectra. The well-known Debye-Scherrer approach has been used to estimate the typical nanocrystallite size (d<sub>c</sub>). The semiconducting nature of glasses has been demonstrated from their DC conductivity. The small polaron hopping process causes nonlinearity in DC conductivity, which is different from AC conductivity. The modified correlated barrier-hopping (CBH) model explains the mechanism of AC conduction. The DC and AC activation energies are found to decrease with the accumulation of TeO<sub>2</sub> in glass matrices.

**Keywords.** Glass nanocomposite; Almond-West formalism; Small polaron hopping; AC and DC Conductivity; Modified CBH model

## 1. INTRODUCTION

Recent years have seen a rise in interest in zinc-phosphate glasses due to its low UV cut-off wavelength, exceptional chemical strength, thermal constancy, and outstanding electrical conduction [1, 2]. Because of their high thermal expansion coefficient, lower melting temperature, and excellent UV transmission, phosphate glasses are of tremendous technological and scientific attention for both practical and theoretical applications [3]. When compared to Pb-based glasses, their weak chemical stability frequently limits their ability for real-world sealing applications. To improve the poor chemical stability of phosphate glasses, the controlled accumulation of oxides such as CuO, MoO<sub>3</sub>, SnO, Sb<sub>2</sub>O<sub>3</sub>, and V<sub>2</sub>O<sub>5</sub> [3] has already been found to be effective.

Due to the remarkable modifications in the physical and structure properties seen in ZnO-P<sub>2</sub>O<sub>5</sub> system, the presence of ZnO into phosphate glasses is quite fascinating [4]. Better chemical stability is achieved by using ZnO such as a network modifier or former, which also results in a wider glass-forming region and lower glass transition temperatures [5]. The glass doped with TeO<sub>2</sub> is challenging to make at large concentrations because of the potential for quick amorphization and phase separation during cooling. As a result, different kinds of defects may occur in TeO<sub>2</sub>-doped glass during the melt quenching procedure. To improve the tellurite glassy network's ability to create glass, metaphosphate can be added [6, 7]. As a result, after being doped with P<sub>2</sub>O<sub>5</sub> as a glass making agent, MoO<sub>3</sub> as a network modifier, and ZnO as network stabilizer, TeO<sub>2</sub>-doped glass can be made utilizing the quench of melt method. Electro-optical applications are made possible by the electrochromism properties and improved ionic conductivity of phosphate glass systems doped with MoO<sub>3</sub>. Mo ions can be found inside glass network as octahedral and tetrahedral structural units because they can exist in two unique valence states, Mo<sup>6+</sup> and Mo<sup>5+</sup> [8, 9]. Due to the development of TeO<sub>4</sub> trigonal bipyramids, doping ZnO-P<sub>2</sub>O<sub>5</sub> glasses with TeO<sub>2</sub> results in changing structural. To determine the most suitable glassy system for more effective applications, we have investigated the results of including both MoO<sub>3</sub> and TeO<sub>2</sub> as mixed modifiers in ZnO-P<sub>2</sub>O<sub>5</sub> glasses in the present work. The purpose of this research is to use the melt quenching method to synthesise three quaternary glassy systems that have the chemical formula 0.60ZnO-0.10P<sub>2</sub>O<sub>5</sub>-0.30[(1-x) MoO<sub>3</sub>-xTeO<sub>2</sub>]. One of the main objectives of this communication is to examine the X-ray diffraction (XRD) patterns to investigate the microstructure. In order to evaluate each sample's semiconducting nature and DC conductivity, the small polaron hopping hypothesis is applied. Almond-West formalism and the well-known Jonscher's Universal Law have both been used to analyze the conductivity of the present glassy systems.

## 2. EXPERIMENTAL PROCEDURE

The unique chemical composition  $0.60\text{ZnO}-0.10\text{P}_2\text{O}_5-0.30[(1-x)\text{MoO}_3-x\text{TeO}_2]$  has been used to synthesize three quaternary glassy nanocomposite systems. ZnO, MoO<sub>3</sub>, P<sub>2</sub>O<sub>5</sub>, and TeO<sub>2</sub> in the proper amount in powder form, all with 99% purity, have been methodically assorted in an alumina crucible according to the stoichiometry of each composition. Initial temperature of the high-temperature electrical furnace is then set to 150°C, and then, it rises at a rate of 10°C/min while the alumina crucible is placed inside the furnace. We cautiously notice the form of the assortment in the furnace every five minutes and record the temperature at which the composite melts. At temperatures between 770°C and 890°C, three samples of quaternary glass ( $x = 0.1, 0.2, \text{ and } 0.3$ ) are melted. The entire melt of each composition has been immediately cooled at 25°C among two superbly polished metal plates in order to form semi-transparent glassy samples with thicknesses of 1-2 mm. To perform the structural measurement, the as-quenched solid glasses are converted into adequate powder form by grinding appropriately. Density ( $\rho$ ) of the as-prepared glasses has been perceived using the Archimedes principle and acetone is used as the immersion liquid. The quaternary glass samples have been tested for density and molecular weight, which are then applied to calculate the molar volumes. An X-ray diffractometer has been used to examine the X-ray diffraction patterns using CuK $\alpha$  radiation. By using the two-probe method and LCR meter, electrical measurements have been conducted. To operate as an electrode, a highly conductive silver paste has been coated on both surfaces of the glass sample. At a range of temperatures, electrical conductivity of glasses has been evaluated in a wide frequency range.

## 3. RESULTS AND DISCUSSIONS

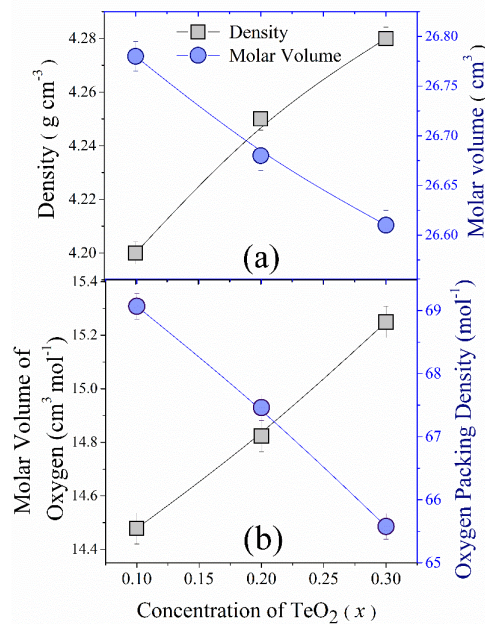
### 3.1. Investigation of Physical Parameters

To determine the nature of structural reforms in amorphous glassy or polycrystalline materials,  $\rho$  is a fundamental characteristic or physical feature. Molecular weight, constituent element fraction, and glass structure type all have a significant impact on oxide glass density. The average values of  $\rho$  of all glasses have been determined using the well-known Archimedes principle (Eq. 1) using the following expression [11].

$$\rho = \left( \frac{W_{air}}{W_{air} - W_{acetone}} \right) \times \rho_{acetone} \quad (1)$$

By applying the derived values of  $\rho$ , the following equation can be employed to determine the molar volume [11].

$$V_M = \sum \frac{x_i \times M_i}{\rho} \quad (2)$$



**Figs. 1(a)** Estimated values of  $\rho$  and  $V_M$ , and **(b)** composition dependence of  $V_O$  and OPD.

As the amount of TeO<sub>2</sub> ( $x$ ) rises, the association between  $V_M$  and  $\rho$  of all examined samples is revealed in Fig. 1(a). TeO<sub>2</sub> and MoO<sub>3</sub> have molecular weights of 159.6 and 143.94 g/mol, respectively. When TeO<sub>2</sub> is added to the glass matrix, the values of  $\rho$  increase as the amount of MoO<sub>3</sub> decreases. The compactness of the glass network increases as the value of  $\rho$

risers, which causes the bond length to decrease as the concentration of TeO<sub>2</sub> rises ( $x$ ) [12]. As the amount of TeO<sub>2</sub> rises,  $V_M$  values decrease, which is also seen in Fig. 1. (a). With the addition of TeO<sub>2</sub>, the decremental bond length and higher stretching force constant produce compact glass structures, which leads to the declining nature of  $V_M$  value [12].

Molar volume of oxygen ( $V_O$ ) and oxygen packing density (OPD) have been assessed in order to better realize the glass structure using associations based on the corresponding values of  $\rho$  and  $V_M$  [13].

$$V_O = \frac{V_M}{\sum_i x_i n_i} \quad (3)$$

and

$$OPD = 1000C \left( \frac{\rho}{M} \right) \quad (4)$$

In the above equations,  $n_i$  is the quantity of oxygen atoms found inside each oxide,  $C$  is the amount of oxygen atoms available within every unit of the formula, and  $M$  is the molecular weight.

For all glass nanocomposites, the computed  $V_O$  and OPD values are shown in Fig. 1(b). TeO<sub>2</sub> is added to the MoO<sub>3</sub>-ZnO-P<sub>2</sub>O<sub>5</sub> glass structure, which results in a reduction in NBO bonds as  $V_O$  rises and OPD falls. This study shows that fewer NBO bonds improve the compactness of glass structure and improve the density of as-prepared glasses [13].

**Table 1:** Several computing parameters from XRD spectra

x (mol%)	2 $\theta$ (Degree) ( $\pm 0.10$ )	FWHM	Identified Phase	h	k	l	$d_c$ ( $\pm 0.06$ )	Crystallinity (%) ( $\pm 0.05$ )
0.15	36.12	0.1903	ZnMoO <sub>4</sub>	0	2	1	31.67	2.21
0.25	31.75	0.1995	Mo <sub>5</sub> TeO <sub>16</sub>	-3	2	1	41.42	3.34
	34.27	0.2123	TeO <sub>3</sub>	1	1	0		
	36.12	0.2003	ZnMoO <sub>4</sub>	0	2	1		
0.35	31.75	0.1874	Mo <sub>5</sub> TeO <sub>16</sub>	-3	2	1	49.65	4.56
	34.27	0.1612	TeO <sub>3</sub>	1	1	0		
	35.45	0.1623	Mo <sub>5</sub> TeO <sub>16</sub>	-3	2	1		
	36.12	0.1887	ZnMoO <sub>4</sub>	0	2	1		

### 3.2. Analysis of XRD Spectra

Glassy systems with TeO<sub>2</sub> doping are shown with their spectra in Fig. 2. Crystallinity can be seen inside the amorphous glassy matrix as evidenced by the distinct peaks and defined widths in the XRD patterns. This leads to the claim that a small number of nanocrystallites are formed within the glassy, amorphous network. The subsequent relation determines the degree of crystallinity for every glassy system and the projected values are presented in Table 1.

$$\% \text{ Crystallinity} = 100 \times \frac{\text{Area of crystalline peak}}{\text{Total area under the patterns}} \quad (5)$$

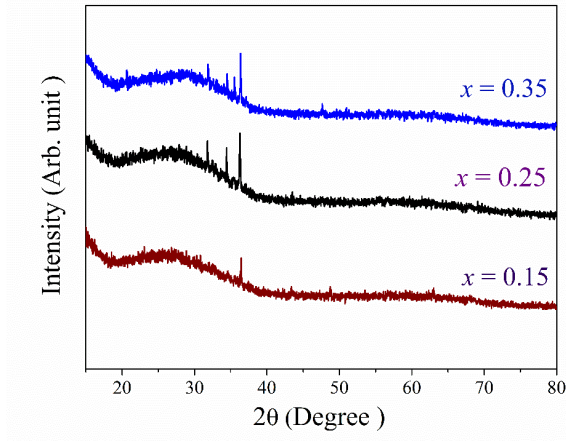
For the effect of the mixed modifier, it has been perceived that the percentage crystallinity values rise as more nanocrystallite phases emerge in zinc phosphate glass matrices. The available literature data has been used to identify and index the nanophases of specific diffraction peaks.

Table 1 demonstrates that the identified nanocrystallites of ZnMoO<sub>4</sub> [14], Mo<sub>5</sub>TeO<sub>16</sub> [15] and TeO<sub>3</sub> [16] are developed within the glassy matrix.

Using the Debye-Scherrer equation, the values of  $d_c$  have been estimated [17].

$$d_c = \frac{0.89\lambda}{\beta \cos \theta} \quad (6)$$

The assessed values of  $d_c$  for all three quaternary glasses are tabulated in Table 1.



**Fig. 2.** Recorded XRD spectra of all glasses

### 3.3. Electrical Conduction Mechanism

This section provides an in-depth assessment of mechanism of electrical conductivity of TeO<sub>2</sub> and MoO<sub>3</sub> doped zinc phosphate glass systems at a wide range of temperatures.

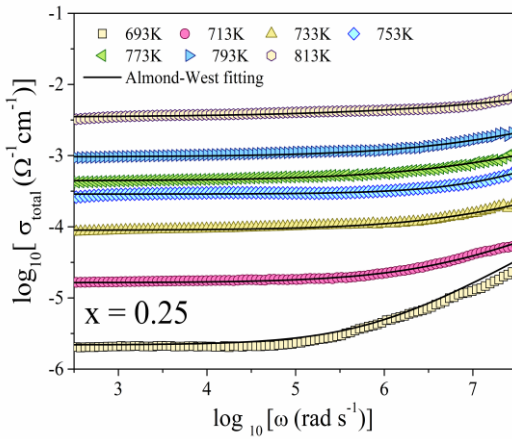


**Fig. 3.**  $\sigma_{total}$  spectra of  $x = 0.25$  glassy system

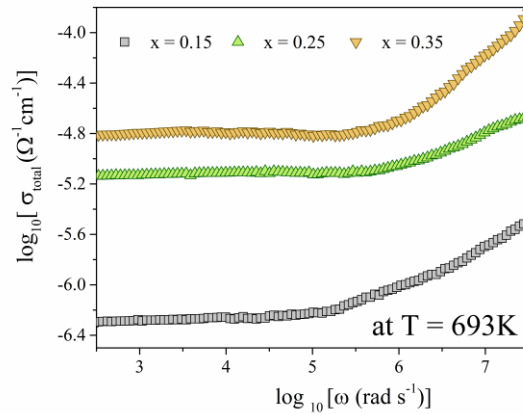


**Fig. 4.**  $\sigma_{total}$  spectra of three quaternary glass systems at  $T = 693K$ .

$\sigma_{total}$  spectra of glass with  $x = 0.25$  and three glasses at a fixed temperature  $T = 693K$  are revealed in Figs. 3 and 4, respectively.

As seen in Figs. 3 and 4, the values of  $\sigma_{total}$  rise as the temperature rises, indicating non-linear properties and the semiconducting characteristics of glasses under investigation. The lower frequency portion has a nearly frequency-independent  $\sigma_{total}$  spectrum (plateau or flat area), which is a property of DC conductivity ( $\sigma_{dc}$ ). The conductivity spectrum displays an almost linear characteristic at higher frequencies.

It is perceived from Fig. 4 that the glass system of  $x = 0.35$  (higher TeO<sub>2</sub> content) reveals higher conductivity.

The Almond-West formalism, which is represented by the succeeding equation, has been used to explore the electrical conduction mechanism of MoO<sub>3</sub> and TeO<sub>2</sub> doped zinc phosphate glass systems [4, 17].

$$\sigma_{total} = \sigma_{dc} \left[ 1 + \left( \frac{\omega}{\omega_H} \right)^p \right] \quad (7)$$

Here, the parameter  $p$  stands for the frequency exponent, and  $\omega_H$  for the crossover frequency. As shown in Fig. 3, curve fitting of entire conductivity data is utilized to assessment of these parameters.

The resultant values of  $\omega_H$  of three quaternary glasses are plotted with inverse of applied temperatures, as shown in Fig. 5(a). The behaviour of temperature dependence is verified in Fig. 5(a), which also demonstrates that the value of  $\omega_H$  rises with temperature. The nature of  $\omega_H$  in a glass according to Arrhenius is explained by the following equation [18].

$$\omega_H = \omega_e \exp\left(-\frac{E_H}{K_B T}\right) \quad (8)$$

The operative attempt frequency is denoted by  $\omega_e$  in the equation above, while the Boltzmann constant is signified by  $K_B$ .

The polaron migration activation energy ( $E_H$ ) for disordered materials is defined as the minimum quantity of energy necessary for small polarons to hop between localized sites that are parted from one another by a potential barrier [18]. In Fig. 5(b), it can be realized that the values of  $\omega_H$  rise as  $\text{TeO}_2$  is added, while  $E_H$  exhibits an inverse relationship with  $\omega_H$ .

The Almond-West formalism yields the values for  $\sigma_{dc}$  that are totally temperature-dependent, and the non-linear behavior of  $\sigma_{dc}$  is caused by the influence of several conduction mechanisms. The subsequent equation can be used to represent the temperature-dependent  $\sigma_{dc}$ .

$$\sigma_{dc} = \sigma_{High} \exp\left(-\frac{E_{High}}{K_B T}\right) + \sigma_{Low} \exp\left(-\frac{E_{Low}}{K_B T}\right) \quad (9)$$

From the equation above, two dissimilar sorts of DC conductivity mechanisms may be inferred:  $\sigma_{dc}$  at high temperatures ( $\sigma_{high}$ ) and  $\sigma_{dc}$  at low temperatures ( $\sigma_{low}$ ). The DC conduction ( $\sigma_{High}$ ) mechanism, which operates at higher temperatures, depends solely on the amount of formed defects states inside the mobility gap, which is determined by the amount of amorphousness in the glassy systems [18].

As opposed to this, the DC conduction ( $\sigma_{low}$ ) mechanism at low temperatures relies on polarons hopping among a variety of produced defects or localized states and relies on the tunnelling mechanism among the nearby potential barriers [19].

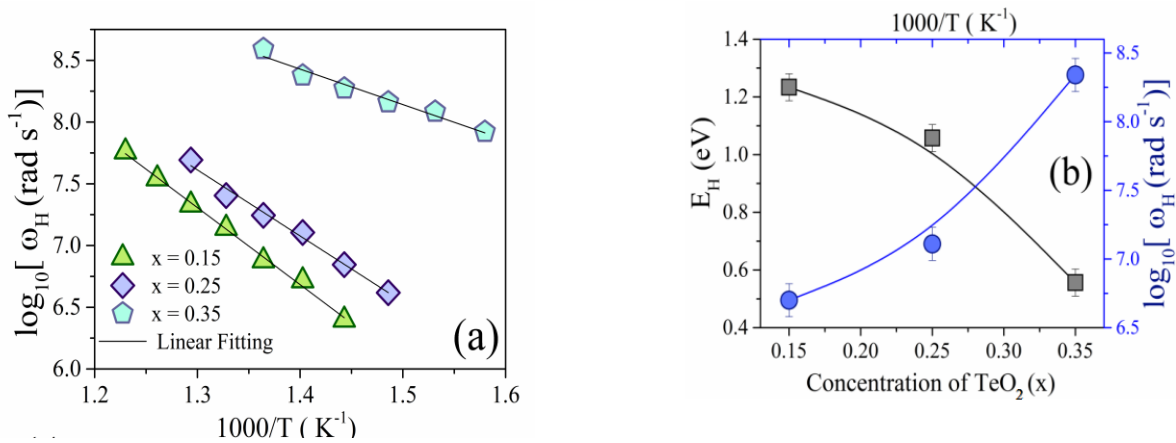


**Fig. 5 (a)** Temperature dependency of  $\omega_H$  and **(b)** composition dependency of  $E_H$  and  $\omega_H$

**Table 2:** Different types of estimated activation energies.

Composition (x, mol%)	Activation energy (DC)		Activation energy (AC)
	$E_{High}$ (eV)	$E_{Low}$ (eV)	$E_{ac}$ (eV)
0.15	2.22	1.31	1.02
0.25	1.87	1.12	0.93
0.35	1.64	0.73	0.74

Fitting with linear equation of the acquired  $\sigma_{dc}$  spectra, as shown in Fig. 6(a), predicts two different types of DC activation energies,  $E_{Low}$  and  $E_{High}$ , for the lower and higher frequency zones, respectively. The values of  $E_{Low}$  and  $E_{High}$  gradually decrease under the impact of  $\text{TeO}_2$  in the  $\text{ZnO-P}_2\text{O}_5$  glassy network, which is supported by the tabulated values of  $E_{Low}$  and  $E_{High}$  in Table 2. As a result, the amount of  $\text{TeO}_2$  increases with the conductivity of the glasses.

The mechanism of AC conductivity of polycrystalline and amorphous glasses is described by the Jonscher universal power-law, which is frequency- and temperature-dependent. [20]

$$\sigma(\omega) = A\omega^s \quad (10)$$

The power-law exponent ( $s$ ) and constant parameter  $A$  are used to calculate the glass system's polarizability strength. The difference between the  $\sigma_{total}$  and the estimated  $\sigma_{dc}$  is subtracted to acquire the AC conductivity ( $\sigma_{ac}$ ) of glasses. Fig. 6(b) establishes the quaternary glass sample's dependence on temperature and frequency. The chance of charge carriers escaping to the conduction state is increased with the rise in temperature due to an increase in lattice vibration. Conduction thus improves, leading to a decrease in activation energy.

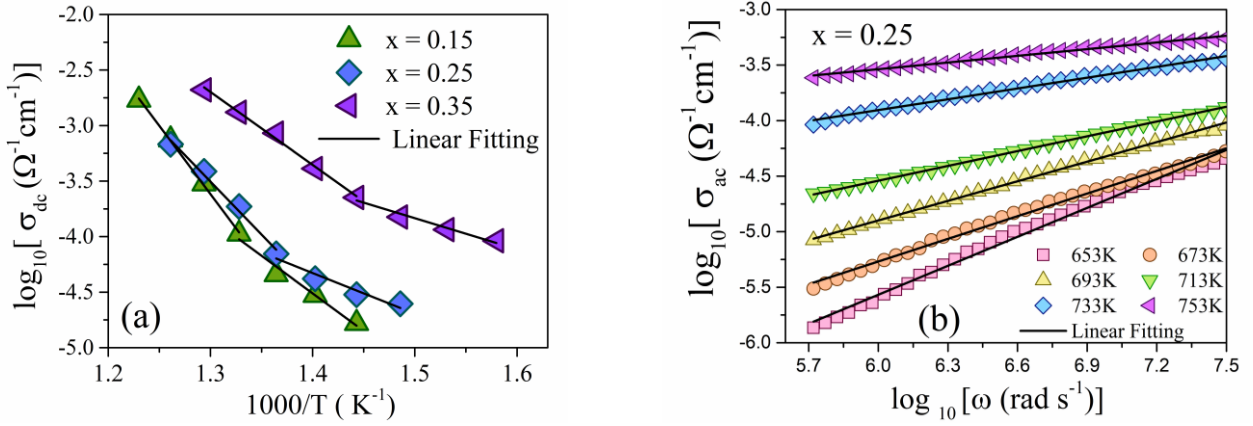


**Fig. 6** (a) Temperature-dependent  $\sigma_{dc}$  of glasses and (b) Frequency-dependent  $\sigma_{ac}$  of glass sample  $x = 0.25$ .

Table 2 provides the activation energies ( $E_{ac}$ ) related to each glass sample's AC conduction mechanism as determined by the fitting with linear equation of the  $\sigma_{ac}$  data. For the glass with  $x = 0.25$ , the alterations in AC with frequency are displayed in Fig. 6(b).  $E_{ac}$  is the necessary energy required for disordered or semiconducting glass to overcome the barrier potential and start the AC conduction process. As  $\text{TeO}_2$  replaces the transition metal oxide  $\text{MoO}_3$ , it has been noticed that the values of  $E_{ac}$  are falling.  $\text{TeO}_2$  content thus improves the AC conduction of the glass system.

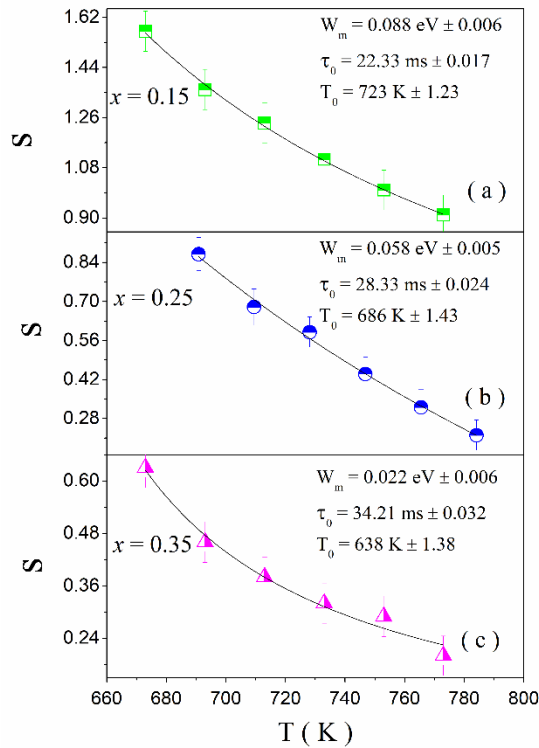


**Fig. 7(a-c)**  $S$  versus  $T$  plots and modified CBH model fittings of all glass samples.

As seen in Fig. 7(a), the temperature dependence of  $\sigma_{ac}$  is projected to occur at higher frequency ranges. The fluctuation of "s" with temperature aids in the adaption of the optimal AC conduction mechanism. According to Fig. 7(a-c), the expected values of "s" for respective glass drop as temperature rises. When "s" declines as temperature rises in disordered or amorphous glassy materials, Pike and Elliott's CBH model offers a precise description of the mechanism of  $\sigma_{ac}$  [17]. As stated in CBH model, conduction occurs as a result of charge carriers (electron or microscopic polarons) hopping over the potential barrier; the amount of energy required to do so is determined by the Coulombic interaction separating the two sites. Jumps between two localized sites are thought to have symmetric jumping possibilities per unit of time, which means they can happen both forward and backward. Little polarons or charge carriers hop when the barrier separating two suitably defined sites is thermally activated.

For glassy systems with greater values of  $s$ , the conventional CBH model is inappropriate. It is important to alter the typical CBH model in the manner described below in order to acquire the correct values for all fitting parameters. [18]

$$s = 1 - \frac{6K_B(T - T_0)}{w_m + K_B(T - T_0) \ln(\omega\tau_0)} \quad (11)$$

As presented in Fig. 7 (a-c), values of fitting parameters hopping barrier potential ( $W_m$ ), Debye relaxation time ( $\tau_0$ ), and ideal thermodynamic temperature of glass transition ( $T_0$ ) are estimated from fitting with modified CBH model (Eq. 11). It has been noted that the  $\sigma_{ac}$  of the glassy system reduces as  $\text{TeO}_2$  content is added to glassy matrices, which causes the values of  $W_m$  to decrease.

#### 4. SUMMARY AND CONCLUSIONS

It is established that the volumetric mass density of all semiconductor glasses having the common formula  $0.60\text{ZnO}-0.10\text{P}_2\text{O}_5-0.30[(1-x)\text{MoO}_3-x\text{TeO}_2]$  prepared by the quenching of melt process increases steadily with increasing of  $\text{TeO}_2$  ( $x$ ) content, while the  $V_M$  decreases since the greater compaction structure of glasses. With the addition of  $\text{TeO}_2$ , the glassy system becomes more compact because the values of  $V_O$  and OPD are continuously increasing and decreasing. The presence of  $\text{ZnMoO}_4$ ,  $\text{Mo}_5\text{TeO}_{16}$ , and  $\text{TeO}_3$  nanocrystallites on amorphous glass matrices is established by XRD patterns. Values of  $d_c$  and the crystallinity (%) both rise with  $\text{TeO}_2$  content. Total conductivity spectra analysis revealed frequency-independent ( $\sigma_{dc}$ ) and frequency-dependent ( $\sigma_{ac}$ ) regions. In both cases, conductivity increased with an increase in temperature due to changes in the bond structures of the glassy systems and the emergence of the defect or localized states, exhibiting semiconductor behavior. The values obtained of the minimum acceptable energy for small polaron migration ( $E_H$ ) and  $E_{ac}$  drop as  $\sigma_{ac}$  rises. The fact that the power-law exponents ( $s$ ) decrease as temperature rises suggests that the AC conductivity mechanism is a perfect match for the modified CBH model. As the AC conductivity rises, the value of the CBH model parameter  $W_m$  drops. According to the findings of the current study, structural changes and conduction processes are significantly influenced by the presence of  $\text{TeO}_2$  and  $\text{MoO}_3$  as mixed modifiers in the glassy matrix of  $\text{ZnO}-\text{P}_2\text{O}_5$ .

#### 5. REFERENCES

- [1] J. Tang, Y. Huang, M. Sun, J. Gou, Y. Zhang, G. li, Y. Kang, J. Yang, Z. Xiao, J. Lumin., "Spectroscopic characterization and temperature-dependent upconversion behavior of  $\text{Er}^{3+}$  and  $\text{Yb}^{3+}$  co-doped zinc phosphate glass", *Journal of Luminescence*, vol. 197 pp. 153–158, 2018
- [2] N. Radouane, A. Maaroufi, B. Ouaki, C. Poupin, R. Cousin, B. Duponchel, D.P. Singh, A.H. Sahraoui, M. Depriester, "Thermal, electrical and structural characterization of zinc phosphate glass matrix loaded with different volume fractions of the graphite particles", *J. Non-Cryst. Solids*, vol. 536, pp. 119989, 2020.
- [3] Y.B. Singh, D. Biswas, S.K. Shah, S. Shaw, R. Mondal, A.S. Das, S. Kabi, L.S. Singh, "Investigation of optical properties and electrical conductivity mechanism of  $\text{Fe}_2\text{O}_3-\text{Sm}_2\text{O}_3-\text{ZnO}-\text{P}_2\text{O}_5$  quaternary glass nanocomposite systems", *Materialia*, vol. 15, pp. 100963, 2021.
- [4] D. Biswas, A.S. Das, R. Mondal, A. Banerjee, D. Deb, A. Dutta, S. Bhattachacharya, S. Kabi, L.S. Singh, "Study of microstructure and electrical conduction mechanisms of quaternary semiconducting glassy systems: Effect of mixed modifiers", *J. Non-Cryst. Solids*, vol. 542, pp. 120104, 2020.
- [5] D. Jain, V. Sudarsan, R.K. Vatsa, C.G.S. Pillai, "Luminescence studies on  $\text{ZnO}-\text{P}_2\text{O}_5$  glasses doped with  $\text{Gd}_2\text{O}_3:\text{Eu}$  nanoparticles and  $\text{Eu}_2\text{O}_3$ ", *J. Lumin. Vol.* 129 (5), pp. 439-443, 2009.
- [6] V.A.G. Rivera, D. Manzani, *Technological Advances in Tellurite Glasses*, Elsevier, vol. 2, pp. 1–100, 2017.
- [7] R.K. Brow, "Review: the structure of simple phosphate glasses", *J. Non-Cryst. Solids*, vol. 263–26, pp. 1–28, 2000.
- [8] P.S. Rao, P.M.V. Teja, A.R. Babu, C. Rajyasree, D.K. Rao, "Influence of molybdenum ions on spectroscopic and dielectric properties of  $\text{ZnF}_2-\text{Bi}_2\text{O}_3-\text{P}_2\text{O}_5$  glass ceramics", *J. Non-Cryst. Solids*, vol. 358, pp. 3372–3381, 2012.
- [9] M.A. Ghauri, S.A. Siddiqi, W.A. Shah, M.G.B. Ashiq, M. Iqbal, "Optical properties of zinc molybdenum phosphate glasses", *J. Non-Cryst. Solids*, vol. 355, pp. 2466–2471, 2009.
- [10] K. Vosejkova, L. Koudelka, Z. Cernosek, P. Mosner, L. Montagne, B. Revel, "Structural studies of boron and tellurium coordination in zinc borophosphate glasses by  $^{11}\text{B}$  MAS NMR and Raman spectroscopy", *J. Phys. Chem. Solid*, vol. 73, pp. 324–329, 2012.
- [11] S. Hassanien, I. Sharma, A.A. Akl, "Physical and optical properties of a-Ge-Sb-Se-Te bulk and film samples: Refractive index and its association with electronic polarizability of thermally evaporated a- $\text{Ge}_{15-x}\text{Sb}_x\text{Se}_{50}\text{Te}_{35}$  thin-films", *J. Non-Cryst. Solids*, vol. 531, pp. 119853, 2020.
- [12] R.K.N. Ningthemcha, D. Biswas, R. Mondal, A.S. Das, S. Kabi, D. Ghosh, L.S. Singh, B. Deb, "Study of mixed modifier effect on dielectric and optical properties of zinc-phosphate based ternary and quaternary nanocomposite systems", *Journal of Non-Crystalline Solids*, vol. 591, pp. 121701, 2022.
- [13] D.P. Singh, G.P. Singh, "Conversion of covalent to ionic behavior of  $\text{Fe}_2\text{O}_3-\text{CeO}_2-\text{PbO}-\text{B}_2\text{O}_3$  glasses for ionic and photonic application", *Journal of Alloys and Compound*. Vol. 546, pp. 224–228, 2013.
- [14] J. Meullemeestre, E. Penigault, *Bull. Soc. Chim. Fr.*, vol. 10 pp. 3669–3674, 1972.

- [15] Y. Arnaud Y, J. Guidot, C. R. Seances Acad. Sci., Ser. C, vol. 282, pp. 631–634, 1976.
- [16] M. Dusek, J. Loub, “X-ray Powder Diffraction Data and Structure Refinement of  $\text{TeO}_3$ ”, Powder Diffraction, vol. 3, pp. 175–176, 1988.
- [17] R.K.N. Ningthemcha, D. Biswas, Y.B. Singh, D. Sarkar, R. Mondal, D. Mandal, L.S. Singh, “Temperature and frequency dependent electrical conductivity and dielectric relaxation of mixed transition metal doped bismuth-phosphate semiconducting glassy systems”, Materials Chemistry and Physics, vol. 249, pp. 123207, 2020.
- [18] D. Biswas, R.K.N. Ningthemcha, A.S. Das, L.S. Singh, “Structural characterization and electrical conductivity analysis of  $\text{MoO}_3\text{-SeO}_2\text{-ZnO}$  semiconducting glass nanocomposites”, J. Non-Cryst. Solids, vol. 515, pp. 21–33, 2019.
- [19] A. Ihyadn, A. Lahmar, D. Mezzane, L. Bih, A. Alimoussa, M. Amjoud, M. El. Marssi, I.A. Luk'yanchuk, “Structural, electrical and energy storage properties of  $\text{BaO-Na}_2\text{O-Nb}_2\text{O}_5\text{-WO}_3\text{-P}_2\text{O}_5$  glass-ceramics system”, Mater. Res. Express, vol. 6, pp. 115203, 2019.
- [20] D. Biswas, A. S. Das, R. Mondal, A. Banerjee, A. Dutta, S. Kabi, L. S. Singh, “Structural properties and electrical conductivity mechanisms of semiconducting quaternary nanocomposites: Effect of two transition metal oxides”, J. Phys. Chem. Solids, vol. 144, pp. 109505, 2020.
- [21] A.K. Jonscher, “Dielectric Relaxation in Solids”, London: Chelsea Di Electrics, pp. 10–152, 1983.

## Biographies



**Arpan Mandal** received the bachelor's degree in Mechanical Engineering from WBUT (MAKAUT) University in 2012, the master's degree in Production Engineering from Jadavpur University in 2017, and the pursuing philosophy of doctorate degree in Mechanical Engineering from Jadavpur University, respectively. He is currently working as a Faculty in the Department of Mechanical Engineering, Regent Education and Research Foundation. His research areas include glass composites.



**Bidyut Kumar Ghosh** received the bachelor's degree in Electrical Engineering from WBUT (MAKAUT) University in 2009, the master's degree in Electrical Devices and Power Systems from WBUT (MAKAUT) University in 2013. He is currently working as a Faculty in the Department of Electrical Engineering, Regent Education and Research Foundation. His research areas are Structural properties of Ionic System, Electrical Conduction and Dielectric relaxation of Ionic system etc.



**Nipu Modak** received the bachelor's degree in Mechanical Engineering from North Bengal University in 2002, the master's degree in Mechanical Engineering Machine Design Specialization from BESU Shibpur in 2004, and the philosophy of doctorate degree in Engineering from Jadavpur University in 2011, respectively. He is currently working as Professor at the Department of Mechanical Engineering, Faculty of Engineering, Jadavpur University. His research areas include Microfluidic transport and separation in MEMS scale application and characteristic analysis of composite, ceramic and nano structured material. He has been serving as a reviewer for many respected journals and conferences.



**Rittwick Mondal** is a post graduate in Physics from Madurai K. University, has a distinguished career of 13 years of teaching Physics in secondary schools, under west Bengal Govt. He has published sixteen research papers in the International SCI journals of repute. His research area includes glass and glassy nanocomposites, Magnetic perovskites, optical properties of mixed former glassy nano composite systems, Green synthesis of Nano particles, and topological analysis of chalcogenide glassy systems. He has been serving as a reviewer for many reputed journals.



**Dr. Dipankar Biswas** is currently working as an Associate Professor in Department of Electronics & Communication Engineering, Regent Education and Research Foundation Barrackpore, West Bengal, India. Having completed his B.E. Degree from University of Burdwan, he started his journey of teaching and research since. Afterwards he completed his M.Tech. from WBUT. And while continuing his teaching and research obsession, he persuaded and got his PhD degree from National Institute of Technology Manipur. Now has more than 16 years of experience teaching in various engineering colleges. Alongside teaching, he has also been indulged in many high-quality researches producing more than 35 high original research articles in various international journals of high repute. His research areas include composite materials, chalcogenide glass, glass ceramic, glucose sensor etc. He has been serving as a reviewer for many reputed journals.